

Numerical Analysis of a Planar O Micromixer with Obstacles

Md. Readul Mahmud*

Department of Physical Sciences, Independent University, Bangladesh (IUB), Dhaka, Bangladesh

Received: May 15, 2022, Revised: June 24, 2022, Accepted: June 25, 2022, Available Online: June 30, 2022

ABSTRACT

Passive mixers rely on the channel geometry to mix fluids and mixing depends primarily on diffusion. However, many previously reported designs either work efficiently only at moderate to high Reynolds numbers (Re) or require a complex 3D channel geometry that is often difficult to fabricate. In this paper, we report the design, simulation, and characterization of a planar O passive microfluidic mixer with two types of obstacles to enhance mixing performance. Numerical investigation on mixing and flow structures in microchannels is carried out using the computational fluid dynamics (CFD) software ANSYS 15 for a wide range of Reynolds numbers from 1 to 200. The results show that the O mixer with obstacles has far better mixing performance than the O mixer without obstacles. The reason is that fluid path length becomes longer due to the presence of obstacles which gives fluids more time to diffuse. For all cases, the O mixer with circular & fin obstacles have 3 times more efficient compared to the O mixer without obstacles. It is also clear that efficiency increase with axial length as expected. Efficiency can be simply improved by adding extra mixing units to provide adequate mixing. The value of the pressure drop is the lowest for the O mixer because there is no obstacle inside the channel. However, the O mixer with circular & fin obstacles has the lowest mixing cost, an important characteristic for integration into complex, cascading microfluidic systems, which makes it the most cost-effective mixer. Due to the simple planar structure and low mixing cost, it can be easily realized and integrated into devices for various macromixing applications.

Keywords: Micromixer, Mixing Efficiency, Mixing Cost, CFD.



This work is licensed under a [Creative Commons Attribution-Non Commercial 4.0 International License](https://creativecommons.org/licenses/by-nc/4.0/).

1 Introduction

Mixing various substances is a typical act of regular day-to-day activity yet it is generally difficult to accomplish good or homogeneous blending. Microdevices and micromixers serve the purpose to obtain excellent mixing on a micro-scale [1]. Micromixers have a high surface-to-volume proportion because of their small dimension, which is a defining characteristic compared to conventional-size chemical process equipment [2]. The flow inside the micromixer is usually laminar due to its small size and mixing usually depends on molecular diffusion at a low Reynolds number [3]. Therefore, good mixing takes a long time and a long channel length. The applications of microdevices and micromixers are increasing daily in various applications such as chemical industry [4], biomedical industry, and biochemical fields [5]-[6]. Micromixers have many advantages such as process safety, low cost to manufacture, less use of chemicals and reagents, better process control, simpler process optimization, rapid design implementation, and easier scale-up through “numbering up” [7]-[11].

Mixers are classified into two types, active and passive [12]-[13]. There are always active parts in active mixers to achieve excellent mixing. On the other hand, passive mixers utilize various channel sizes and lengths, and unique geometric configurations to compensate for the absence of active elements [14]. The passive mixer increases the contact area between fluids and promotes molecular diffusion. Active mixers are mainly divided into electrodynamic, electrodynamic, dielectrophoretic, magnetic, acoustic, time-pulse, pressure perturbation, thermal, and other types [15]-[16].

T shape and Y shape mixers are the oldest mixers designed and analyzed by researchers. Many authors have investigated the detailed design and working principle of T-shaped micromixers in recent years [14],[17]-[20]. Numerical and/or experimental

flow regimes, the influence of secondary flow, vortex flow, and mixing performance have been computed extensively [8],[21]-[23] recently. Generally, the T mixer provides poor efficacy at low Reynolds numbers due to the laminar nature of flow (also the absence of advection). Hence various obstacles or grooves are placed inside the mixers which creates chaotic advection and as a result increases the efficiency. Many authors introduce various size and shape of obstacles in T mixers which increase efficacy but results in high-pressure drop [24]-[27]. Four passive micromixer designs (G1, G2, G3, and G4) and G1 and G4 designs provided a high mixing due to the presence of chaotic advection [28]. A T mixer having staggered fins has been numerically studied for a set of parametric (spacing of fins, angle of inclination, Reynolds number, and width of fins) [29]. A simple O-type mixer is presented and analyzed experimentally by Nimafar et. al. [30] for low Reynolds number ($0.08 < Re < 4.16$). The incremental mixing efficiency is about 81% and 17.6% at $Re=0.803$ and $Re=4.166$, respectively after 15 mm along the channel length.

Mixers based on baffles and obstacles have been investigated by several groups and involve varying the overall channel geometry [31]-[33]. Bhagat et. al. [34] tested with Circular, triangular, and diamond obstructions which increase the efficiency for the value of Re equal to 1. Both Shim et. al. [35], and Chung and Shih [36] incorporated a variety of diamond obstructions into their respective designs which yield high efficiency at Re of 200.

SAR (split and recombine) mixers effectively reduce the diffusion length, increase the surface contact area between two fluids and as a result increase the efficiency. SAR mixers of various geometrical shapes and sizes are examined by many researchers [37]-[38]. Generally, SAR mixers provide good efficiency but have high pressure drop due to their complex structure.

In recent years, ridges and grooves are introduced to achieve chaotic mixing. In chaotic-advection micromixers, 3D channel structures [39]-[40], and planar design [32],[41] were used to enhance fluid mixing. Stroock et. al. [42] proposed herringbone-shaped grooves which yield high efficiency (90%) at a low Reynolds number.

In this present work, a simple O-shaped mixer is studied. To improve the performance of the O mixer with circular obstacles and a combination of circular & fin obstacles are introduced. The main goal is to optimize the mixer by investigating the effects of obstruction geometry and shape. Numerical simulation is performed to compute fluid flow, fluid concentration, mixing index, and pressure drop by ANSYS Fluent 15 for $1 \leq Re \leq 200$. To validate the simulation setup, numerical data is compared with published experimental results. Finally, the best performing mixer is proposed based on the overall performance.

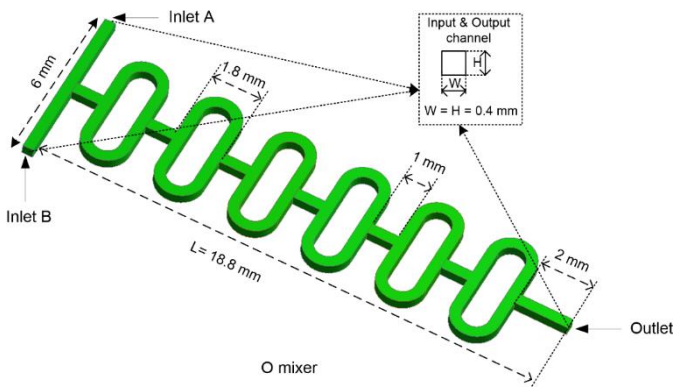


Fig. 1 Simple O mixer

2 Design of Micromixers

The geometry of an O mixer is investigated by Nimafar et al. [30] as shown in Fig. 1. The inlet channels and output channels present a square cross-section with an aspect ratio of 1:1, i.e., $W = H = 0.4 \text{ mm}$.

Two types of obstacles are introduced inside the O mixer to enhance the mixing index. Circular-shaped obstacles and a combination of circular & cylindrical fin-shaped obstacles are placed inside the O mixer. The diameter of circular-shaped obstacle (d) is 0.2 mm. The length and width of the fin obstacle (s) are 0.3 mm and 0.07 mm, respectively. All examined mixers consist of 6 identical elements connected one after another and the total length is 18.8 mm (one element is 2.8 mm long). Detail configuration of the obstacles in the O mixer is represented in Fig. 2.

3 Numerical Setup and Methodology

The fluid dynamic study was accomplished using the computational code ANSYS Fluent 15. The fluid is considered incompressible, with steady-state, isothermal, and laminar flow conditions. The flow field is solved using continuity, Navier-Stokes, and advection-diffusion equations as given below [43]-[44],

$$\nabla \cdot V = 0 \quad (1)$$

$$\rho V \nabla \cdot V = -\nabla P + \mu \nabla^2 V \quad (2)$$

$$V \cdot \nabla C = D \nabla^2 C \quad (3)$$

Where V is the fluid velocity (m/sec), ρ is the fluid density (Kg/m^3), P is the fluid pressure (Pa), μ is the fluid viscosity

($\frac{Kg}{m \cdot sec}$), C is the fluid molar concentration (mol/m^3), and D is fluid diffusivity (m^2/sec).

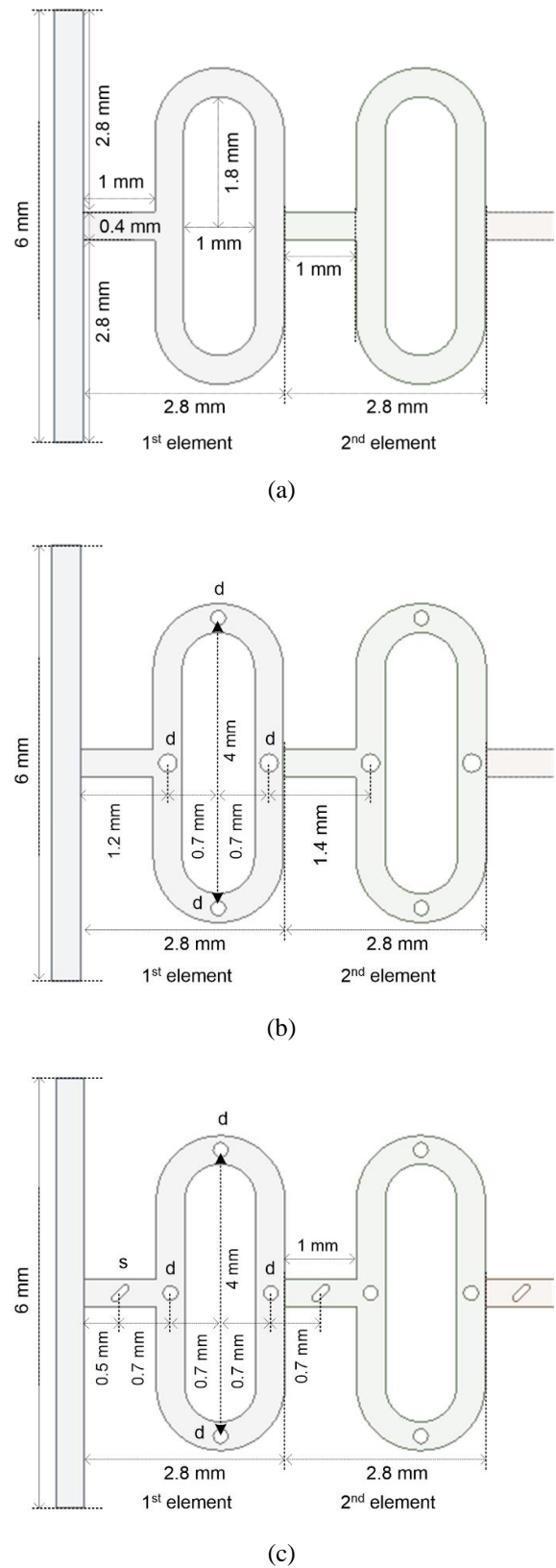


Fig. 2 Two elements of the O mixer, the O mixer with circular obstacles, and the O mixer with circular & fin obstacles

In the numerical simulation, the no-slip velocity condition at all walls is considered, the uniform flow velocity is employed at both inlets (Inlet A and Inlet B as shown in Fig. 1), and the output

is set to zero (0) gauge pressure. It is assumed that Fluid A (flowing through Inlet A) has a relative species concentration of one (1) and Fluid B (flowing through Inlet B) has zero (0). The two input fluids are considered to have the same properties as water at 20°C with density $\rho = 998.2 \text{ Kg/m}^3$, dynamics viscosity $\mu = 0.001 \text{ Pa s}$ and diffusivity $D = 1 \times 10^{-9} \text{ m}^2/\text{s}$ [5]. The coupling of pressure–velocity is solved via the SIMPLE (Semi Implicit Method for Pressure Linked Equations) method [7]. Whereas a second-order upwind scheme is employed for momentum and species concentration. The convergence criteria for continuity, momentum, and species transport equations are used with scaled residuals of 1×10^{-6} in this study. An important dimensionless parameter called Reynolds number (Re) is computed [45].

$$Re = \frac{\rho V d}{\mu} \quad (4)$$

$$d = \frac{2WH}{W + H} \quad (5)$$

Where Re is the Reynolds number, d is the characteristics hydraulic diameter (m), W is the width of the mixing channel (m) and H is the height of the mixing channel (m).

The mixing index is calculated using the following equations [46],

$$\sigma = \sqrt{\frac{1}{N} \sum_{i=1}^N (C_i - C_{av})^2} \quad (6)$$

$$\eta = 1 - \frac{\sigma}{\sigma_{max}} \quad (7)$$

Where, C_i is the concentration at the i^{th} node, C_{av} is average concentration, σ is the standard deviation, and σ_{max} is the maximum standard deviation ($\sigma_{max} = 0.5$). Maximum and minimum efficiency can be zero ($\eta = 0$) and one ($\eta = 1$), respectively.

Mixing efficiency and pressure drop alone is not sufficient to have a complete comparison among various mixers. Hence, mixing cost is computed by using pumping power which is used to flow liquid inside the mixer by following the equation [12]-[13], [47],

$$M_c = \frac{\Delta P Q}{\eta} \quad (8)$$

Where M_c denotes the mixing cost (*watts*), ΔP is the pressure drops (Pa), Q is the flow rate (m^3/s) and η is the efficiency.

3.1 Meshing

The numerical results always depend on the mesh system; hence grid independence tests were carried out to find a suitable number of grids. The structured grids with hexahedral elements have been employed for all mixers by Fluent 15. Fig. 3 shows an example of the grid system of the O mixer and O mixer with circular & fin obstacles.

Fig. 4 shows the grid dependency of the O mixer with circular & fin obstacles for five different numbers of nodes from 2.20×10^6 to 6.97×10^6 . The mixing index was calculated along the axial length of the mixer at $Re = 10$.

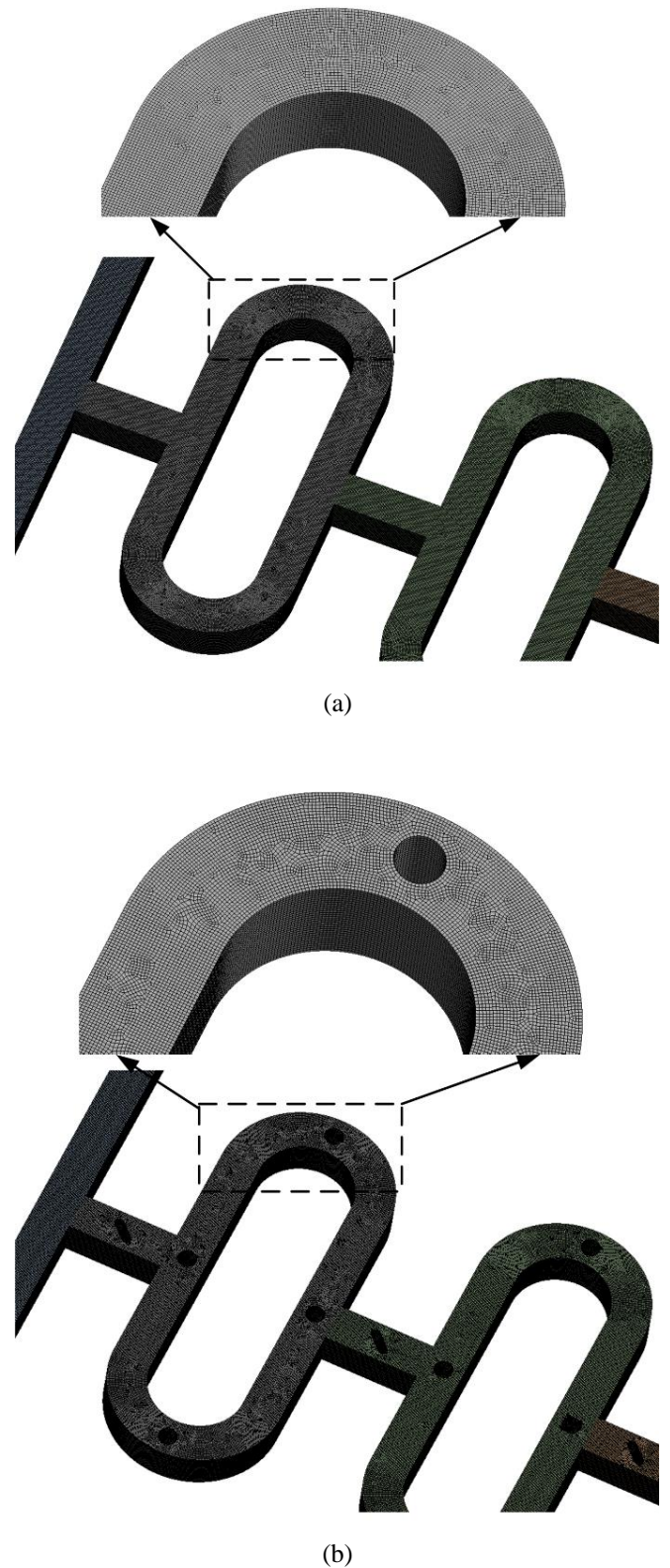


Fig. 3 Hexagonal grids inside the (a) O mixer and the (b) O mixer with circular & fin obstacles

Accurate grid setting is a crucial part of numerical simulation. The mixing efficiency decreases as the number of grids increases as represented in Fig. 4. However, the variation is very small (maximum 2.4%) between nodes of 5.48×10^6 and 6.97×10^6 nodes. Hence 5.48×10^6 nodes are used for further analysis of the O mixer with obstacles which will cost-effectively provide acceptable numerical data.

Similarly, 5.30×10^6 nodes and 5.33×10^6 nodes of mesh were used for the O mixer with circular obstacles and the O mixer with circular & fin obstacles, respectively.

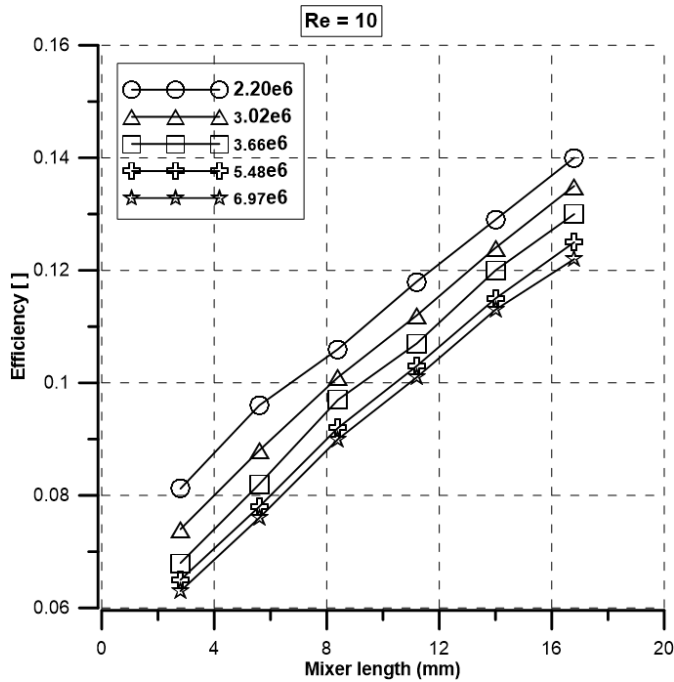


Fig. 4 Mixing efficiency along the axial length of the O mixer at $Re = 10$

3.2 Numerical Validation

To validate the numerical simulation, published experimental results are compared with numerical simulation. To have a preliminary qualitative comparison, the image of mixing in the O mixer experimentally and numerically is demonstrated in Fig. 5 at Reynolds numbers equal to 4.166. Blue and yellow colors indicate two input fluids and two fluids mixed along the channel. The numerical result shows improper mixing of species, which is in good agreement with the experimental results.

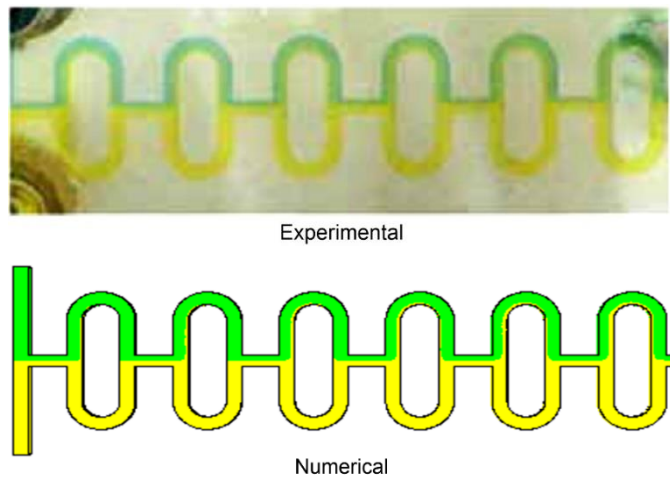


Fig. 5 Concentration distribution through the O mixer in experimental method [30] and numerical method at $Re = 4.166$

To have a qualitative comparison, the numerical mixing efficiency of the O micromixer is compared with the published experimental result [30] as shown in Fig. 6. Both curves have a maximum value at $Re = 0.083$ and then decreases with the increase of Reynolds numbers. The maximum difference

between the experimental and numerical results is less than 9%. The discrepancy is primarily due to several reasons. Firstly, the number of nodes in the numerical simulation was kept within a certain limit due to the computational limitation as well as to reduce simulation cost. Secondly, there may be variations in dimension and smoothness between the numerical and actual models. Lastly, the experimental efficiency was computed using images of the top view mixing, while the numerical values are obtained from the cross-sections of the outlet.

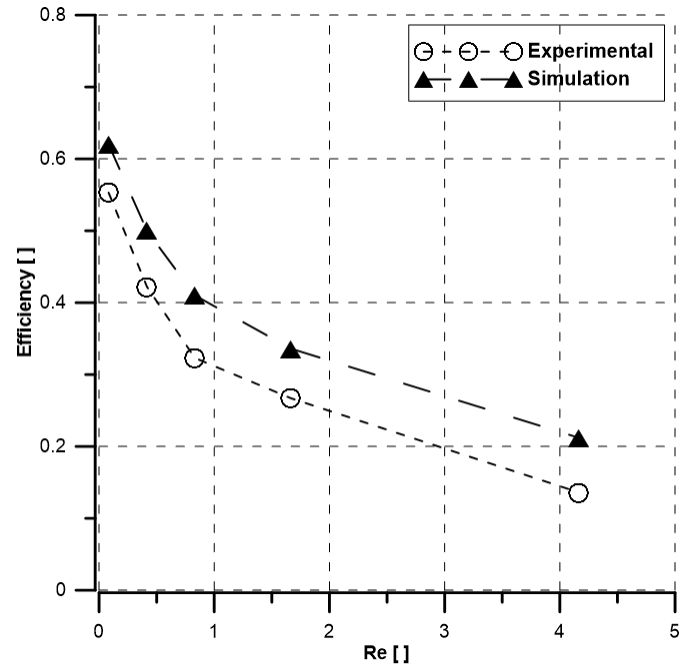


Fig. 6 Comparison of numerical results and experimental values [30] after 15 mm along the axial length of the O mixer

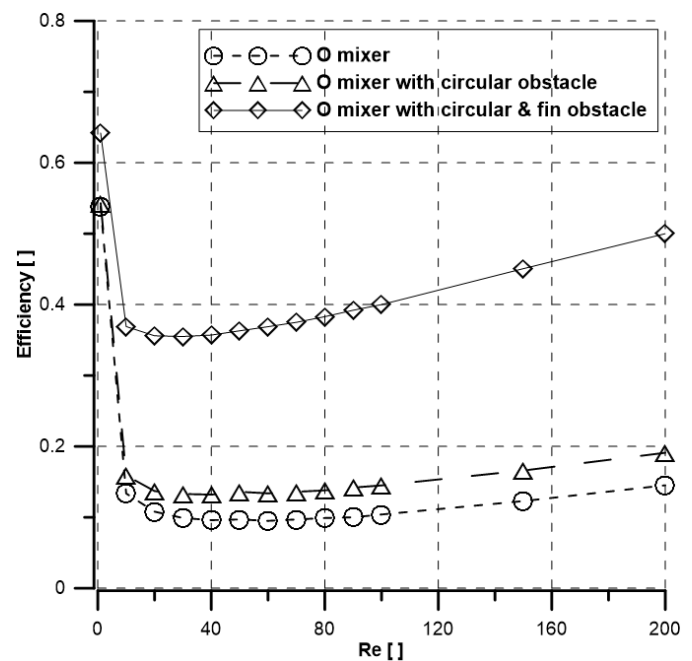


Fig. 7 Mixing efficiency at the output of the mixers at various Reynolds numbers

4 Results and Discussion

The performance of the three mixers was evaluated numerically for Reynolds numbers from 1 to 200. The mixing efficiency obtained for all three mixers is presented in Fig. 7. Fig.

8 presents the water distribution along the channel for various Reynolds numbers for all three mixers. All mixers show efficiency of more than 50% at $Re \leq 1$. At low Reynolds numbers, usually at $Re \leq 1$, molecular diffusion dominant the mixing process, and fluids have longer residence times resulting in high mixing efficiency. For channels with micromixers, at moderate Reynolds numbers ($1 < Re \leq 10$), fluids have less time to mix and resulting poor efficiency as evident in Fig. 7 and Fig. 8. Efficiency starts to increase as the Reynolds numbers increase after $Re > 10$. In this case, the mixing time decreases

with the increase of Reynolds numbers (flow rate), but fluids path becomes longer due to split and recombination of fluids which compensates for the shorter mixing time as shown in Fig. 8. This effect is more evident in the case of the O mixer with circular & fin obstacles and mixing efficiency is the highest (about 50%). Whereas the efficiency is about 15% and 20% for the O mixer and the O mixer with circular obstacles at $Re = 200$, respectively. In addition, the O mixer with circular & fin obstacles yields three times more efficiency than the other two at all examined Reynolds numbers.

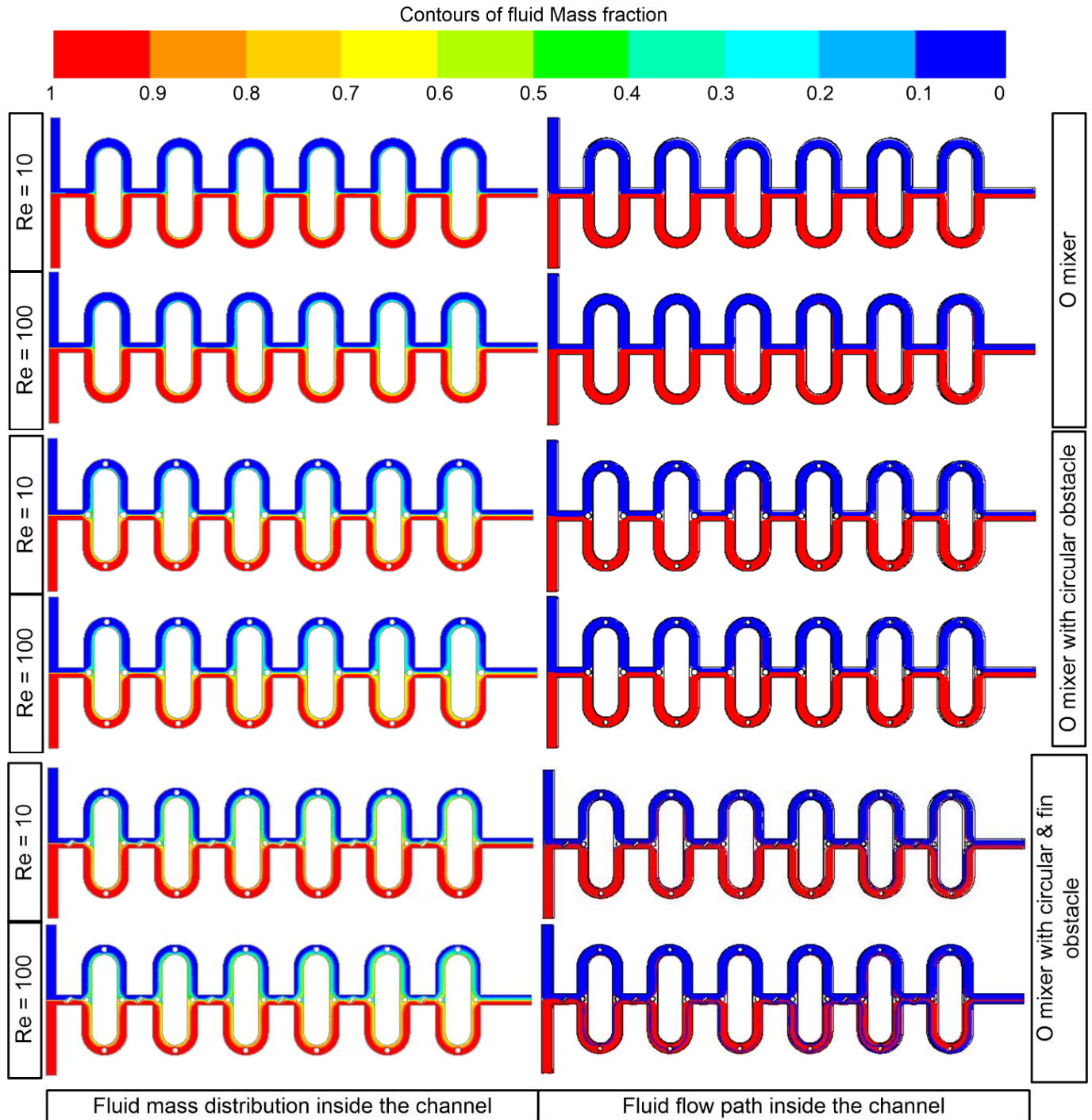


Fig. 8 Fluid mass fraction contours at a mid-plane (left) and fluid path (right) inside the mixers

The fluid mass fraction inside the three mixers at $Re = 1$ and $Re = 10$ is presented in Fig. 9. It is evident that the fluids' mass fraction is closer to the ideal value (0.5) at $Re = 1$ which indicates good mixing (over 50% efficiency). As the Reynolds numbers ($Re = 10$) increases the homogeneity decreases as the mass fraction moves away from the ideal value which predicts low efficiency as confirmed in Fig. 7.

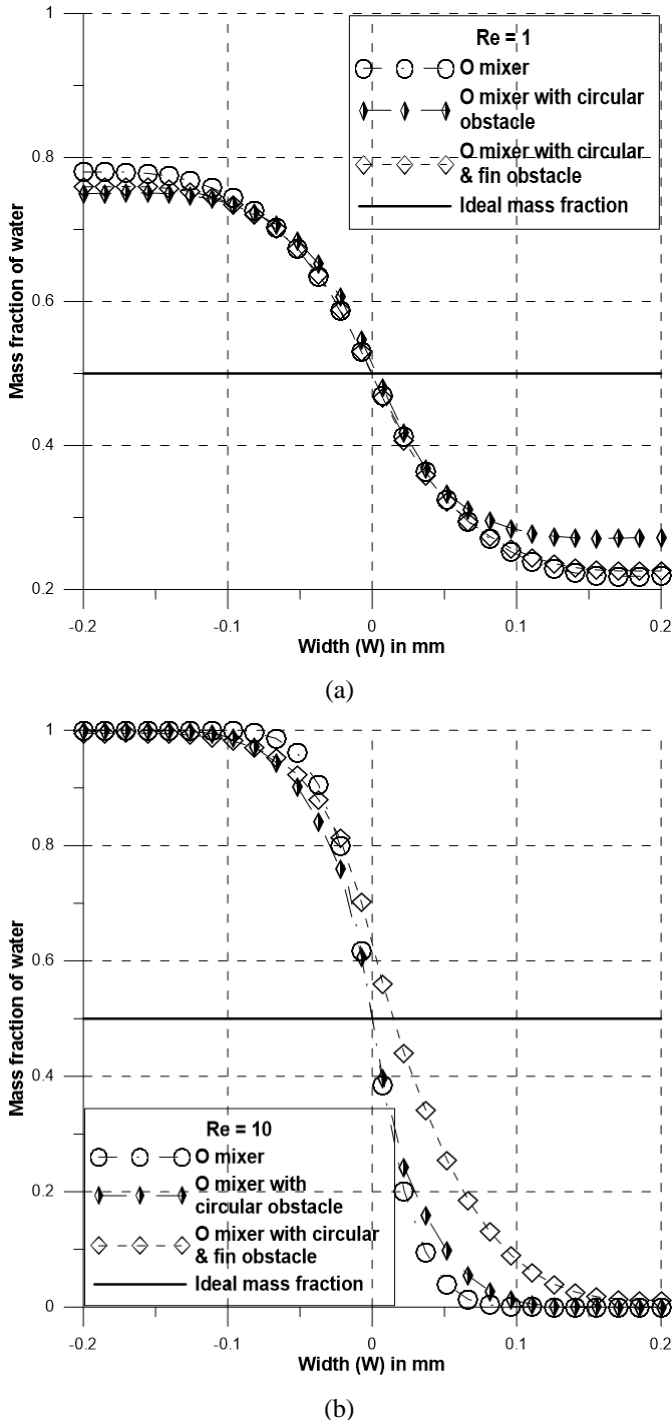


Fig. 9 Distributaries of mass fraction of water along the horizontal mid-line ($z = 0.02$ mm) at the outlet of the mixers for (a) $Re = 1$ and (b) $Re = 10$.

The O mixer without obstacles and the O mixer with circular obstacles show close results at all examined Reynolds numbers because the circular obstacles alone have a minor effect to increase the path length of fluids. Hence the fluids do not have enough time to diffuse as illustrated in Fig. 8. On the other hand,

the O mixer with circular & fin obstacles bends and tangled the fluids path enough to lengthen the mixing path which increases the residence time and results in higher efficiency. Therefore, at high Reynolds numbers ($Re = 200$) the O mixer with circular & fin obstacles yields 50% efficiency whereas the O mixer and the O mixer with circular obstacles show an efficiency of 15% & 20%, respectively.

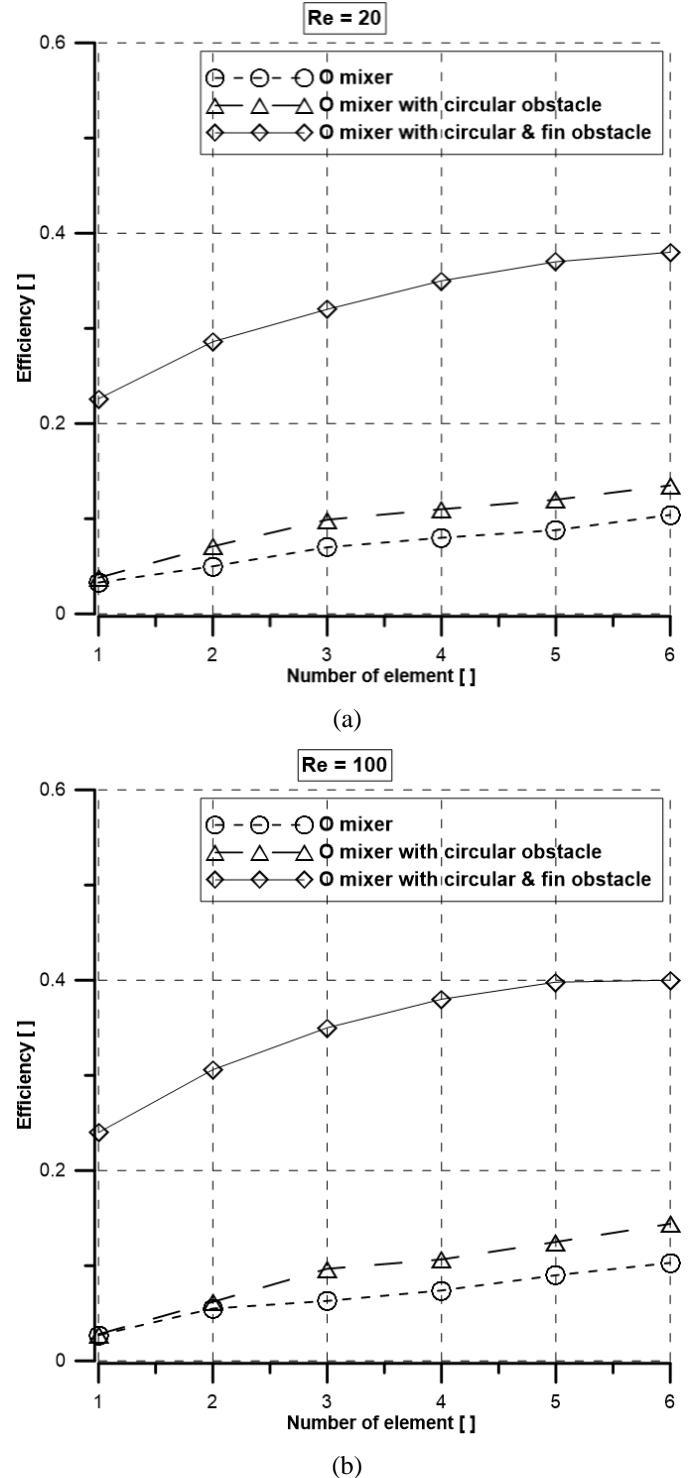


Fig. 10 Mixing efficiency variation to the number of elements at (a) $Re = 20$ and (b) $Re = 100$

The O mixer consists of a repetitive connection of O shaped segment which is called an element. In this study, the O mixer consists of six O-shaped elements. Mixing efficiency is calculated after each element along the channel and the

efficiency after each element at $Re = 20$ and $Re = 100$ is presented in Fig. 10. The O mixer without obstacle shows the lowest efficiency as expected. The O mixer with circular & fin obstacles presents the highest mixing efficiency because fluids have more time to diffuse due to the increase in path length. Desire percentage of efficiency can be achieved by adding more elements to the mixers.

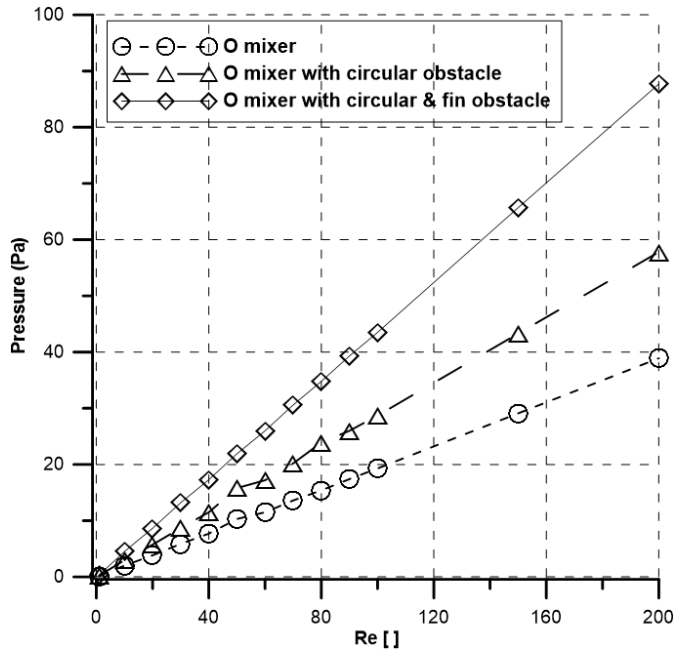


Fig. 11 Pressure-drop at the outlet of the mixers at various Reynolds numbers

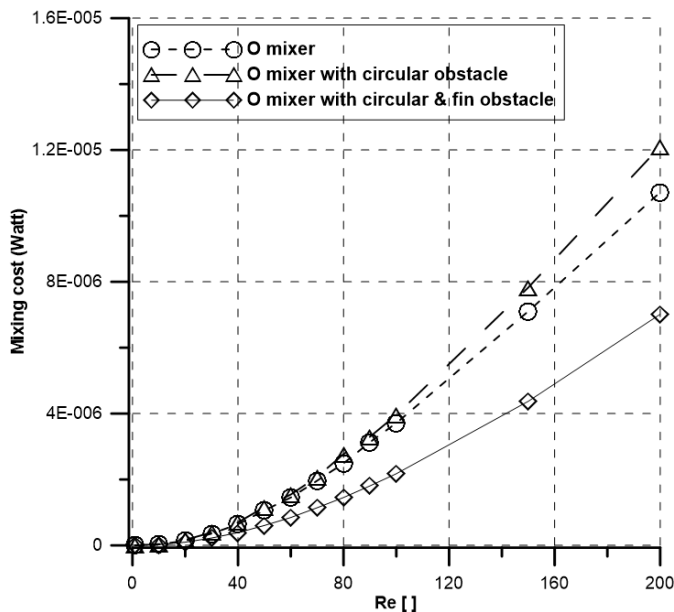


Fig. 12 Mixing cost of the mixers at various Reynolds numbers

Fig. 11 presents the pressure drop versus Reynolds numbers for all three mixers. Pressure drop increases with the increase of Reynolds numbers for all mixers. The O mixer yields the lowest pressure drop due to the absence of obstacles and the O mixer with circular & fin obstacles yields the highest pressure drop. Mixing efficiency and pressure drop alone is not sufficient to suggest the best performing mixer. Therefore, a parameter called mixing cost is evaluated (using equation (8)) and demonstrated in Fig. 12. The O mixer with circular obstacles shows the highest

mixing cost due to its low efficiency (almost equal to the O mixer) and moderate pressure drop compared to the three mixers. Whereas the mixing cost of the O mixer with circular & fin obstacles presents the highest pressure drop and efficiency but the ratio is the lowest, hence mixing cost is the lowest. Therefore, the O mixer with circular & fin obstacles is the best performing mixer with the highest mixing efficacy and the lowest mixing cost.

5 Conclusion

In this study, two types of obstacles (circular obstacles and circular & fin obstacles) are introduced to a planar O mixer. Numerical simulation was performed to evaluate the effect of obstacles on fluid flow, mixing performance, and pressure drop using the ANSYS 15 commercial software at a wide range of Reynolds numbers ($1 \leq Re \leq 200$). The numerical results showed good agreement with the experimental and present good mixing performance over a wide range of flow conditions, particularly in the low Re ($Re=1$) and high Re ($Re=200$). The presented design is planar, and obstructions are all full channel height, thus can be constructed in a simple fabrication process. The introduction of circular and fin obstacles inside the O mixer increases the efficacy three times compared to the O mixer without obstacles, and a maximum of 50% efficiency can be achieved with only six elements. Efficiency also increases with the increase of elements for all three mixers. Desire efficiency can be obtained by adding elements in series. Though the pressure drop of the O mixer with circular and fin obstacles are high, the mixing cost is the lowest due to its high efficacy. Finally, it can be proposed that the O micromixer with circular and fin obstacles is the best performing one which can be easily realized and integrated with microfluidic systems due to the simple planar structure.

References

- [1] Rahmamezhad, J. and Mirbozorgi, S.A., 2019. CFD analysis and RSM-based design optimization of novel grooved micromixers with obstructions. *International Journal of Heat and Mass Transfer*, 140, pp.483-497.
- [2] Adeosun, J.T. and Lawal, A., 2009. Numerical and experimental studies of mixing characteristics in a T-junction microchannel using residence-time distribution. *Chemical Engineering Science*, 64(10), pp.2422-2432.
- [3] Shah, I., Kim, S.W., Kim, K., Doh, Y.H. and Choi, K.H., 2019. Experimental and numerical analysis of Y-shaped split and recombination micro-mixer with different mixing units. *Chemical Engineering Journal*, 358, pp.691-706.
- [4] Engler, M., Kockmann, N., Kiefer, T. and Woias, P., 2004. Numerical and experimental investigations on liquid mixing in static micromixers. *Chemical Engineering Journal*, 101(1-3), pp.315-322.
- [5] Schikarski, T., Trzenschiok, H., Peukert, W. and Avila, M., 2019. Inflow boundary conditions determine T-mixer efficiency. *Reaction Chemistry & Engineering*, 4(3), pp.559-568.
- [6] Shi, X., Huang, S., Wang, L. and Li, F., 2021. Numerical analysis of passive micromixer with novel obstacle design. *Journal of Dispersion Science and Technology*, 42(3), pp.440-456.
- [7] Mouheb, N.A., Malsch, D., Montillet, A., Sollic, C. and Henkel, T., 2012. Numerical and experimental investigations of mixing in T-shaped and cross-shaped micromixers. *Chemical engineering science*, 68(1), pp.278-289.
- [8] Hoffmann, M., Schlüter, M. and Rübiger, N., 2006. Experimental investigation of liquid-liquid mixing in T-shaped micro-mixers using μ -LIF and μ -PIV. *Chemical engineering science*, 61(9), pp.2968-2976.
- [9] Dundi, T.M., Raju, V.R.K. and Chandramohan, V.P., 2019. Characterization of mixing in an optimized designed T-T mixer with cylindrical elements. *Chinese Journal of Chemical Engineering*, 27(10), pp.2337-2351.

- [10] Wong, S.H., Ward, M.C. and Wharton, C.W., 2004. Micro T-mixer as a rapid mixing micromixer. *Sensors and Actuators B: Chemical*, 100(3), pp.359-379.
- [11] Shamloo, A., Vatankhah, P. and Akbari, A., 2017. Analyzing mixing quality in a curved centrifugal micromixer through numerical simulation. *Chemical Engineering and Processing: Process Intensification*, 116, pp.9-16.
- [12] Mondal, B., Mehta, S.K., Patowari, P.K. and Pati, S., 2019. Numerical study of mixing in wavy micromixers: comparison between raccoon and serpentine mixer. *Chemical Engineering and Processing-Process Intensification*, 136, pp.44-61.
- [13] Gidde, R., 2022. On the study of teardrop shaped split and collision (TS-SAC) micromixers with balanced and unbalanced split of subchannels. *International Journal of Modelling and Simulation*, 42(1), pp.168-177.
- [14] Raza, W., Hossain, S. and Kim, K.Y., 2020. A review of passive micromixers with a comparative analysis. *Micromachines*, 11(5), p.455.
- [15] Lee, C.Y., Chang, C.L., Wang, Y.N. and Fu, L.M., 2011. Microfluidic mixing: a review. *International journal of molecular sciences*, 12(5), pp.3263-3287.
- [16] Nguyen, N.T. and Wu, Z., 2005. Micromixers - A review. *Journal of Micromechanics and Microengineering*, 15(2), pp.1-16.
- [17] Cai, G., Xue, L., Zhang, H. and Lin, J., 2017. A review on micromixers. *Micromachines*, 8(9), p.274.
- [18] Lee, C.Y., Wang, W.T., Liu, C.C. and Fu, L.M., 2016. Passive mixers in microfluidic systems: A review. *Chemical Engineering Journal*, 288, pp.146-160.
- [19] Barabash, V.M., Abiev, R.S. and Kulov, N.N., 2018. Theory and practice of mixing: A review. *Theoretical Foundations of Chemical Engineering*, 52(4), pp.473-487.
- [20] Lee, C.Y. and Fu, L.M., 2018. Recent advances and applications of micromixers. *Sensors and Actuators B: Chemical*, 259, pp.677-702.
- [21] Bothe, D., Stemich, C. and Warnecke, H.J., 2008. Computation of scales and quality of mixing in a T-shaped microreactor. *Computers & Chemical Engineering*, 32(1-2), pp.108-114.
- [22] Bothe, D., Lojewski, A. and Warnecke, H.J., 2011. Fully resolved numerical simulation of reactive mixing in a T-shaped micromixer using parabolized species equations. *Chemical engineering science*, 66(24), pp.6424-6440.
- [23] Galletti, C., Roudgar, M., Brunazzi, E. and Mauri, R., 2012. Effect of inlet conditions on the engulfment pattern in a T-shaped micro-mixer. *Chemical Engineering Journal*, 185, pp.300-313.
- [24] Tseng, L.Y., Yang, A.S., Lee, C.Y. and Hsieh, C.Y., 2011. CFD-based optimization of a diamond-obstacles inserted micromixer with boundary protrusions. *Engineering Applications of Computational Fluid Mechanics*, 5(2), pp.210-222.
- [25] Fang, Y., Ye, Y., Shen, R., Zhu, P., Guo, R., Hu, Y. and Wu, L., 2012. Mixing enhancement by simple periodic geometric features in microchannels. *Chemical Engineering Journal*, 187, pp.306-310.
- [26] Ansari, M.A., Kim, K.Y. and Kim, S.M., 2018. Numerical and experimental study on mixing performances of simple and vortex micro T-mixers. *Micromachines*, 9(5), p.204.
- [27] Santana, H.S., Silva Jr, J.L., Tortola, D.S. and Taranto, O.P., 2018. Transesterification of sunflower oil in microchannels with circular obstructions. *Chinese journal of chemical engineering*, 26(4), pp.852-863.
- [28] Lameu da Silva Junior, J., Haddad, V.A., Taranto, O.P. and Silva Santana, H., 2020. Design and analysis of new micromixers based on distillation column trays. *Chemical Engineering & Technology*, 43(7), pp.1249-1259.
- [29] Tan, S.J., Yu, K.H., Ismail, M.A. and Teoh, Y.H., 2020. Enhanced liquid mixing in T-mixer having staggered fins. *Asia-Pacific Journal of Chemical Engineering*, 15(6), p.e2538.
- [30] Nimafar, M., Viktorov, V. and Martinelli, M., 2012. Experimental investigation of split and recombination micromixer in confront with basic T-and O-type micromixers. *Int. J. Mech. Appl*, 2(5), pp.61-69.
- [31] Bhagat, A.A.S. and Papautsky, I., 2008. Enhancing particle dispersion in a passive planar micromixer using rectangular obstacles. *Journal of micromechanics and microengineering*, 18(8), p.085005.
- [32] Menegeaud, V., Josserand, J. and Girault, H.H., 2002. Mixing processes in a zigzag microchannel: finite element simulations and optical study. *Analytical chemistry*, 74(16), pp.4279-4286.
- [33] Shih, T.R. and Chung, C.K., 2008. A high-efficiency planar micromixer with convection and diffusion mixing over a wide Reynolds number range. *Microfluidics and Nanofluidics*, 5(2), pp.175-183.
- [34] Bhagat, A.A.S., Peterson, E.T. and Papautsky, I., 2007. A passive planar micromixer with obstructions for mixing at low Reynolds numbers. *Journal of micromechanics and microengineering*, 17(5), p.1017.
- [35] Shim, J.S., Nikcevic, I., Rust, M.J., Bhagat, A.A.S., Heineman, W.R., Seliskar, C.J., Ahn, C.H. and Papautsky, I., 2007, January. Simple passive micromixer using recombinant multiple flow streams. In *Microfluidics, BioMEMS, and Medical Microsystems V (Vol. 6465, pp. 300-307)*. SPIE.
- [36] Chung, C.K. and Shih, T.R., 2008. Effect of geometry on fluid mixing of the rhombic micromixers. *Microfluidics and Nanofluidics*, 4(5), pp.419-425.
- [37] Bessoth, F.G., deMello, A.J. and Manz, A., 1999. Microstructure for efficient continuous flow mixing. *Analytical communications*, 36(6), pp.213-215.
- [38] Lee, S.W., Kim, D.S., Lee, S.S. and Kwon, T.H., 2006. A split and recombination micromixer fabricated in a PDMS three-dimensional structure. *Journal of micromechanics and microengineering*, 16(5), p.1067.
- [39] Liu, R.H., Stremmer, M.A., Sharp, K.V., Olsen, M.G., Santiago, J.G., Adrian, R.J., Aref, H. and Beebe, D.J., 2000. Passive mixing in a three-dimensional serpentine microchannel. *Journal of microelectromechanical systems*, 9(2), pp.190-197.
- [40] Yuan, S., Zhou, M., Peng, T., Li, Q. and Jiang, F., 2022. An investigation of chaotic mixing behavior in a planar microfluidic mixer. *Physics of Fluids*, 34(3), p.032007.
- [41] Wong, S.H., Bryant, P., Ward, M. and Wharton, C., 2003. Investigation of mixing in a cross-shaped micromixer with static mixing elements for reaction kinetics studies. *Sensors and Actuators B: Chemical*, 95(1-3), pp.414-424.
- [42] Stroock, A.D., Dertinger, S.K., Ajdari, A., Mezic, I., Stone, H.A. and Whitesides, G.M., 2002. Chaotic mixer for microchannels. *Science*, 295(5555), pp.647-651.
- [43] Mariotti, A., Galletti, C., Mauri, R., Salvetti, M.V. and Brunazzi, E., 2018. Steady and unsteady regimes in a T-shaped micro-mixer: Synergic experimental and numerical investigation. *Chemical Engineering Journal*, 341, pp.414-431.
- [44] Cortes-Quiroz, C.A., Azarbadegan, A. and Zangeneh, M., 2017. Effect of channel aspect ratio of 3-D T-mixer on flow patterns and convective mixing for a wide range of Reynolds number. *Sensors and Actuators B: Chemical*, 239, pp.1153-1176.
- [45] Orsi, G., Roudgar, M., Brunazzi, E., Galletti, C. and Mauri, R., 2013. Water-ethanol mixing in T-shaped microdevices. *Chemical Engineering Science*, 95, pp.174-183.
- [46] Viktorov, V., Mahmud, M.R. and Visconte, C., 2016. Design and characterization of a new HC passive micromixer up to Reynolds number 100. *Chemical Engineering Research and Design*, 108, pp.152-163.
- [47] Tayeb, N.T., Hossain, S., Khan, A.H., Mostefa, T. and Kim, K.Y., 2022. Evaluation of Hydrodynamic and Thermal Behaviour of Non-Newtonian-Nanofluid Mixing in a Chaotic Micromixer. *Micromachines*, 13(6), p.933.